

ZnO, TiO₂ and Ag nanoparticles impact against some species of pathogenic bacteria and yeast

Asmmaa Khalis Mohammed¹, Khonaw Kader Salh^{1*}, Fattma A. Ali^{2*}¹ College of Medicine, Hawler Medical University, Erbil, Kurdistan Region-Iraq² College of Health Science, Hawler Medical University, Erbil, Kurdistan Region-Iraq

*Correspondence to: Fattima.ali@hmu.edu.krd, khonaw.kaderi@hmu.edu.krd

Received July 18, 2021; Accepted September 9, 2021; Published November 22, 2021

Doi: <http://dx.doi.org/10.14715/cmb/2021.67.3.4>

Copyright: © 2021 by the C.M.B. Association. All rights reserved.

Abstract: The economic approaches for manufacturing the nanoparticles with physical and chemical effects and limited resistance to antibiotics have been progressed recently due to the rise of microbial resistance to antibiotics. This research aimed to study the antimicrobial efficacy of silver nanoparticles Ag, ZnO, and TiO₂ nanoparticles against *Salmonella typhimurium* and *Brucella abortus* and *Candida albicans*. Two isolates of *Salmonella* and two isolates of *Brucella abortus* were isolated from food spastically meat and blood specimens, respectively. *Candida albicans* were isolated from the patient's mouth with oral candidiasis (oral thrush) and confirmed diagnosis by API 20C test. The antimicrobial susceptibility of *Salmonella typhimurium* and *B. abortus* isolates were performed against nine different antibiotics. Silver nanoparticles consisting of AgNPs size (90) nm, ZnO NPs size (20, 50) nm as well as TiO₂ NPs size (10, 50) nm, were used. UV-Visible spectrophotometer was used to characterize silver nanoparticles. The highest resistance of *Candida albicans* was seen for fluconazole, Clotrimazole and Itraconazole. The results of the Minimum Inhibitory Concentration (MIC) of nanoparticles against *Salmonella typhimurium* showed the average MIC of TiO₂-10nm and TiO₂-50nm were 5000 and 2500 µg/ml for S1 and S2 isolates, respectively. The isolated *Brucella abortus* (B1 and B2) showed sensitivity to NPs with different MIC. The average MIC for Ag-90nm was 5000 and 2500 µg/ml for B1 and B2 isolates, respectively. The findings suggest NP solution has fungicidal and bactericidal impacts on the tested microorganisms so they can be suitable for multiple applications of the biomedical field such as developing new antimicrobial agents.

Key words: ZnO; Ag; TiO₂ nanoparticle; Antibacterial properties; Antifungal activity.

Introduction

The increasing bacterial resistance to multiple antibiotics has raised the demand for alternative antimicrobial agents. In this regard, to avoid antibiotic use, scientists have been interested in nanoparticles, a nanoscale material ranging from 1-100 nanometers (1). The metal oxide nanomaterials possess antimicrobial activity over a wide range of both Gram-positive and Gram-negative bacteria, including resistant bacterial strains. Iron oxide (Fe₃O₄), zinc oxide (ZnO), magnesium oxide (MgO), copper oxide (CuO), and titanium dioxide (TiO₂) nanoparticles are well-known nanomaterials with high antimicrobial properties (2). This potency of antibacterial activity might be attributed to the generation of reactive oxygen species (ROS) as their intrinsic photocatalytic activity or the metallic ions release (3).

According to World Health Organization (WHO) report, non-typhoidal *Salmonella* represents one of the major etiological agents of infectious diseases worldwide (4). Multidrug resistance non-typhoidal *Salmonella* emergence worldwide is a critical public health issue, for which severe problems would be generated for the treating intestinal and extra-intestinal infection complications (5). Multidrug resistance is associated with enhanced virulence due to the rapid global spread of these multidrug-resistant non-typhoidal *Salmonella* strains

among human societies (6). Additionally, based on research conducted in Denmark, the mortality rate was reported higher in patients who have an infection due to multidrug-resistant *Salmonella typhimurium* compared to those caused by sensitive strains (7). Surprisingly, there is a discriminating advantage for resistance *Salmonella* in the environment where extra amounts of antibiotics are used because the antibiotic treatment itself acts as a risk factor for infection with the resistant bacteria (8).

Antibiotics with penetrating ability to macrophages are preferred for brucellosis treatment. Consequently, brucellosis relapsing is seen not due to anti-*Brucella* drug resistance but because of microorganisms' ability to last inside host cells away from the antibiotics. Thus, antibiotics with intracellular activity are considered effective tools in managing brucellosis (9). As a result of increasing therapeutic failure, relapses, toxicity, and side effects of the conventional antibiotic regimen, searching for new medications has been raised during recent years (10).

Candida is a ubiquitous eukaryotic yeast residing in healthy individuals as a part of the normal microbial flora of the skin, gastrointestinal tract, and genitourinary tract. The risk of developing opportunistic *Candida* infections increases when host immunity is compromised. The most common species associated with *Candida* in-

fections is *Candida albicans* (11), often manifested as oral thrush, vulvovaginitis cutaneous candidiasis (12). National Committee has published recent guidelines for macro-and microdilution assay for in vitro testing of antifungal susceptibilities for Clinical Laboratory Standards (NCCLS) (13). These tests showed a well in vitro correlation (14).

Nano antibiotics (nanomaterial possessing antimicrobial properties) could act as an alternative to fighting against multi-drug resistant organisms (15). Silver nanoparticles (Ag NPs), because of their antiviral and antibacterial properties, are known as the most promising nano-antibiotics (16). For several decades' silver has been used as a disinfectant agent. Inclusive, silver nitrate has been used for treating burns and infection control. However, due to the discovery of penicillin, the use of silver as an antimicrobial agent has been reduced. Currently, the increasing resistance to antifungal agents has attracted attention to silver as an antibiotic once again.

Among nanosized metal oxides, zinc oxide (ZnO), due to its attractive properties such as high surface-to-volume ratio, low cost, and long-term environmental stability, has gained much attention (17). Several studies have already reported that ZnO nanoparticles are non-toxic to human cells and toxic to bacterial cells. Toxicity studies showed that DNA in human cells is not damaged by zinc ions; a property that makes ZnO nanoparticles biocompatible with human cells.

The aims of this study were the isolation of (*Salmonella typhimurium*, *Brucella abortus*, and *Candida albicans*) from food and different clinical specimens, and identification of the isolated bacteria by rapid method serological, via VITEK2 systems. In addition to assessing the activity of conventional antimicrobial activity against these different pathogens compared with the effects of nanoparticles in different sizes (ZnO and TiO₂ and Ag) with an antibiotic-resistant pathogen.

Materials and Methods

Isolation and bacterial identification (*Salmonella typhimurium* and *Brucella abortus*)

Two isolates of *Salmonella* were isolated from food spastically meat. The enrichment phase in the selective

liquid environment was carried out using Rappaport Vassiliadis Broth, which is considered as a selective enrichment for detecting *Salmonella* spp. from foods (18). The goal of this step was to increase the growth and vitality of the bacteria. Rappaport Vassiliadis (V.R.) broth was used through the transfer of 0.1 ml of the second diluents to a tube containing 9 ml of sterile broth and incubated for 18-24 hrs in the presence of 5–10% CO₂. At 37 °C, 0.1 ml of the broth was transferred to the surface of XLD media and incubated for 18-24 h. The two isolates of *Brucella abortus* were isolated from blood specimens and cultured using a BACTEC automated blood culture system (9050; Becton & Dickinson, Franklin Lakes, NJ, USA). The specimens were incubated at 37 °C for 7 to 30 days and were sub-cultured in Mueller Hinton plus 5% blood and *Brucella* agar plates. Rose Bengal and 2-mercaptoethanol (2-ME) agglutination serological tests were performed to detect *Brucella* antibodies. In addition to the Conventional Biochemical tests, the VITEK-2 system (19) [bioMe 'rieux] was used according to McFadden (20).

2- Isolation of fungi: fungi, especially *Candida albicans*, were isolated from patients' mouths, who had oral candidiasis (oral thrush) by sterile swabs containing transported media. After inoculation on Sabouraud's Dextrose agar and incubation for 48hrs at 37 °C, in addition to the API 20C test (21) (Merieux Bio) and germ tube were used to them. Oral *Candida* colonization is usually displayed through a microscopic examination using potassium hydroxide (KOH) or fungal cultures.

Susceptibility to antibacterial agents

The antimicrobial susceptibility of *S. typhimurium* and *B. abortus* isolates were performed against nine different antibiotics (22). For this purpose, the disc diffusion method was recruited according to the Clinical and Laboratory Standards Institute instruction (23). The antibiotic discs used in this study were (Becton Dickinson Co, Maryland, USA): Ampicillin (AM/10 µg), Gentamicin (G.M./10 µg), Chloramphenicol (C/30 µg), Amikacin (AK/30 µg), Nitrofurantoin (NIT/300 µg), Rifampin (FEP/30 µg), Imipenem (IPM/10 µg), Ceftriaxone (CRO/30 µg) to evaluate antimicrobial susceptibility for both two strains of each *S. typhimurium* and *B. abortus* respectively Table1. The discs impregnated

Table 1. Detection of susceptibility to antibacterial agents.

Antibiotic discs	Isolated bacteria							
	S1		S2		B1		B2	
	Inhibition zone (mm)	Patterns of sensitivity	Inhibition zone (mm)	Patterns Of sensitivity	Inhibition zone (mm)	Patterns Of sensitivity	(mm)	Patterns Of sensitivity
Cefoxitin (FOX 30)	≤ 2	R	1	R	0.012	R	0	R
Gentamycin (GN 30)	≤ 4	S	2,5	S	4	S	0	S
Chloramphenicol (IC300)	4	S	3.25	S	1.25	S	4	S
Amikacin (AK 30)	0.25	R	0.07	R	0.2	R	0	R
Ceftriaxone (CRO 30)	2.0	R	≤ 4	R	2.5	S	3	S
Nitrofurantoin (NIT300)	0	R	0	R	0	R	0	R
Rifampin FEP 30	2.2	S	2	S	0.75	R	0.5	R
Ampicillin (AM10)	0.19	R	≤ 1	R	2.4	S	8	S
Imipenem (IPM10)	0.2	R	0	R	0	R	0	R

with antibiotics were placed using sterile forceps. The effect of the antibiotics was tested in each dish. Then the petri dishes were incubated bottom up for 18–24 h at 37 °C. The results were assessed by the presence of inhibition zones around the disks. Test organism growth inhibition at a distance from the disc with the antibiotic was indicative of the strain's susceptibility. If the test organism developed close to the disk with antibiotics, this organism was determined as resistant to the antibiotic CLSI 2006, M 100-S16).

Preparation of nanoparticles

Silver nanoparticles consisted of AgNPs size (90 nm), ZnO NPs size (20,50) nm as well as TiO₂NPs size (10,50) nm, were used. The M. K Impex Corporation-Canada Company has set some qualities to manufacture silver nanoparticles. The particles should be measured at 20 nm with a molecular weight of 107.87 g / mol. The density should be 10.49 g / ml with a purity of 99.95%. Powder grey color, and shape of spherical product chemical way and space superficial density of 20 g/m² but silver nanoparticles measuring 90 nm with a purity of 99.9 % and the item is received from the company in the form of plastic explosive 25 g capacity. ZnO N.P.s was in the form of powder, reaching the size (20) nm and purity 99.9% white color powder, molecular weight 81.39 g / mol density 5.610 g / ml. The company has prepared multiple plastic containers containing one of which 100 g, and for the TiO₂NPs measuring 10 nm has been received in the form of nanopowder, measuring nanoparticles as 10nm and an area of the shallow grave of 225 g / m², the degree of purity of 99%, moisture 0.48%, TiO₂ NPs measuring 50 nm and a degree purity of 99%.

According to the method, a stock solution was prepared (24). One hundred mg of nanoparticle powders added to 10 ml of deionized water next shaking vigorously to break the mass for a homogeneous solution in 5 minutes and then sterilized at 121°C for 20 minutes, cooled at room temperature to get a final concentration of stocks 10 mg/ml.

UV-visible spectrophotometer

UV-Visible spectrophotometer (Thermo Scientific-NanoDrop1000 lab tech international) was used to characterize silver nanoparticles. The Scientific research center/Salahaddin University's device at 400-800nm helped characterize silver nanoparticles (25).

FTIR analysis

The powders were characterized using the FTIR spectrometer (Shimadzu) at a wavelength between 4000-400cm⁻¹ (26).

Antimicrobial activity of nanoparticles

Broth Dilution Method: A prerequisite way used for quantitative assessment to demonstrate the impact the effectiveness of nanoparticle using microtiter plate 96 holes, and conducted depending on the method as follows (27):

100 ul of Mueller Hinton broth was added to each well. 2. 100 ul of nanoparticle prepared at concentration 5000 ug /ml was added to No. 1 well within the pit row A. has been blending the counter through the use of

micropipette and withdrawing grown to several times (6-8) and this made any weakness diluted concentration equivalent to 2500 micrograms/ml. 3. 100 ul of well 1 was transformed to well two and blended the same way to form a dilution with a concentration of 1250 ug/ml. 4. Repeated process down to well No. 10 and then pull them 100 ul and neglected and thus we get the concentrations (625,312.5, 156.25, 78.125, 39.06, 19.53, 9.76 ug/ml). 5. The micro-titer plate was covered and incubated at 37 °C for (24-18) hours. 6. The MIC of nanoparticles is determined by the lowest concentration that withdraw the observable growth of bacteria. The indication of microorganism's growth in control tubes was examined by tube turbidity.

Agar well-diffusion method

The standard agar well diffusion method was used to investigate nanoparticles' antibacterial effects (28). For culturing the bacteria and fungus, Mueller-Hinton agar medium and potato dextrose agar medium were used respectively to test antimicrobial activity by agar well diffusion method against pathogenic microorganisms *S. typhimurium*, *B. abortus*, and *C. albicans*. The pure cultures of pathogens were prepared in 10 ml of nutrient broth followed by overnight shaking at 37° C. Each strain was swapped homogeneously onto the individual Muller-Hinton and potato dextrose agar using sterile cotton swabs [CLSI, 2009:29(3)]. The six wells by sterile, boring cork (5 mm diameter) puncture. The 5 mm well was impregnated with different concentrations of each Ag 90, ZnO 20,50, NPs, and TiO 20,50. For making No.6 to well negative control, distal water was added to it and incubated at 37°C for 24hrs. The process was repeated three times. To determine the inhibitory growth of the NPs on the specific pathogen, the mean value was taken into consideration (29).

Antifungal disk paper preparation

All antifungal drugs were obtained in powdered form. A stock solution of each drug using dimethyl sulfoxide (except fluconazole in sterile double distilled water) was prepared by applying 20µl of an appropriate dilution of the test solution to 6 mm in diameter of Whatman filter paper No.1 (30) as follows: Fluconazole (10 µg), Ketoconazole (30 µg), Clotrimazole (10 µg), Voriconazole (1µg), and Amphotericin-B (20 µg). According to the antifungal potency of (Rosco Diagnostica company), they were taken out and allowed to dry under aseptic conditions and stored at °C in a refrigerator.

Antifungal susceptibility testing

The disk dissemination method was used to test antifungal susceptibility. As the "CLSI" (M44-A) procedures, the inoculum was set up by picking five particular colonies from a 24 hr old *Candida* species culture. Colonies were suspended in 5ml of sterile 0.9% normal saline. The suspension was vortexed to get uniform turbidity and adjusted visually to 0.5 McFarland standards. The suspension was injected into "Mueller Hinton Glucose Agar containing 2% glucose. Moreover, 0.5 µg/ml of methylene blue was used for susceptibility testing. Antifungal disks are placed so that they are not closer than 24 mm from the center. The plates were located in an incubator at 37 °C for 24 hr. The inhibition zone

Table 2. Inhibition zone of different antifungal against *Candida albicans*.

Antifungal	Zone inhibition C1 (mm)	Zone inhibition C2 (mm)	Sensitive mm	Resistance mm
Amphotericin-B Paper disk 20µg	21 (S)	20 (S)	≥15	<10
Clotrimazole paper disk 10 µg	4 (R)	5 (R)	≥ 20	≤ 11
Voriconazole paper disk 10 µg	18 (S)	21 (S)	≥17	≤13
Itraconazole paper disk 10 µg	6 (R)	6 (R)	≥16	≤ 9
Fluconazole paper disk 10 mg	5 (R)	3 (R)	≥19	≤13
Ketoconazole paper disk 10 µg	8 (R)	10 (R)	≥ 30	≤ 22

diameter was measured in millimeters using a ruler for a separately antifungal disk. Clarification of entirely antifungal susceptibility (Susceptible S and resistant R) was made according to (CLSI M44A standards, 2009) (Table 2).

Results and Discussion

The automated VITEK 2 compact system was the final step to identify *Brucella abortus* using Gram-negative bacteria code according to the manufacturer's instructions, which checked 47 biochemical tests and one as a negative control thoroughly. *B. abortus* differentiated by their requirement to CO₂, H₂S production and positive in ILATk (L-lactate alkalization), the food samples were examined using Rappaport Vassiliadis Broth found non-typhoid Salmonella, it enriches salmonellae especially *S. typhimurium* because they can multiply at relatively lower pH compared to other gut bacteria. Rappaport Vassiliadis Broth has a p.H. around 5.2. Also identified by their ability to grow, colonies may range from clear to pink /red. Most colonies 2-4 mm with black centers on XLD agar ferment glucose and produce (gas, H₂S). For obtaining the sera, both of the clotted blood samples were centrifuged at 3,000 × g for 10 min, and 2-mercaptoethanol (2-ME) agglutination tests were performed to perceive Brucella antibodies. Titers higher than 1:40 were considered positive for 2-ME tests based on reference. The primary commercial product used for testing medically significant yeasts was the original API 20C yeast identification strip with index code. One of the reactions which gave results for all the isolates tested were: glucose (+), 2-keto-glutarate (+), inositol (-), cellobiose (-), lactose (-), maltose (+), raffinose (-), and galactose (+). Along with other morphological features, a creamy round colony on SDA allowed the identification of *Candida* species. The reactions were confirmed by the germ tube after incubating *Candida* with 0.5ml human serum for 3 hrs at 37 °C, and 10% KOH showed positive.

This study generally demonstrated the antimicrobial susceptibility of *S. typhimurium* and *B. abortus* isolates against nine different antibiotics. The results indicated *B. abortus* as the most multidrug resistance isolated bacteria that phenotypically showed sensitivity to only three antibiotics, including Ampicillin, Chloramphenicol, gentamicin, and represented resistance to six antibiotics Cefoxitin, ciprofloxacin, imipenem, and rifampicin Amikacin respectively. At the same time, isolates of *Salmonella* were resistant to carbapenems (Imipenem), β-lactams (cefotaxime, Ceftriaxone), aminoglycosides (Amikacin), and Gentamycin. *Salmonella typhimurium* and *Brucella abortus* were resistant to β-lactams (Ceftriaxone, Cefoxitin), aminoglycosides (amikacin), imi-

penem and susceptible to Gentamycin and Chloramphenicol, as presented in Table 1. These results align with the growing rates of antimicrobial resistance among non-typhoidal *Salmonella*, highlighting the caution in using these antibiotics (31).

Standard first-line therapy for *Salmonella* infections is based on Chloramphenicol, sulfa drugs, Ampicillin, and fluoroquinolone. In this case, all of these antibiotics would be unsuccessful, if the *Salmonella* was a multidrug-resistant strain, and treatment will be brutal. A former statement designates death in the patients subsequently, a nosocomial *Salmonella* epidemic in a U.S. hospital (32).

Fluoroquinolones, trimethoprim/ sulfamethoxazole, and Ampicillin are well-known as typical first-line therapy for *Salmonellosis*. The emergence of resistance to these antibiotics in non-typhoidal *Salmonella* represents a severe problem in treating infections due to these organisms (33). A discriminating advantage could be well-thought-out for resistant *Salmonella* in the environment where unnecessary antibiotics are used, and the antibiotic therapy itself is an important risk factor for infection with resistant bacteria (8).

A rapid increase has been seen in microbial resistance to common antibiotics, signaling the urgent need for new antibiotics classes to treat many infectious diseases. The WHO declared that only a few antibiotics are clinically efficient and have good intracellular penetration for brucellosis treatment (34). The results revealed that both *B. abortus* isolates were phenotypically resistant to Cefoxitin, Amikacin, Nitrofurantoin, Imperium, and Rifampicin. These results are inconsistent with those reported by Gattringer *et al.* (2010), who found out that REP Rifamycin had remarkable bactericidal activity at a low concentration (35). Bacterial RNA and protein synthesis could be blocked by Rifamycins and result in a noticeable bactericidal effect inside and outside the cell. However, some patients are prevented from using RIF for an extended period because of the apparent gastrointestinal reaction. Yet, an alternative medication or combined use of additional drugs should be used to reduce patients' discomfort.

Indeed, the excitation of several metabolic processes can also contribute to rifampin resistance in *Brucella* (36). This study showed variable antibiotic susceptibility of the bacterial isolates to gentamicin, Ampicillin, Ceftriaxone, and, Chloramphenicol. As the most effective antibacterial agent (37), Ceftriaxone is described with a high outcome on bacteria in idiophase and mostly performances on the bacterial cell wall. Still, it does not affect the ongoing cell wall synthesizing in the inactive condition. While there are only preliminary case reports on the handling of *Brucella* infection by gentamicin or Ampicillin (38), AMP, and aminoglycosides medica-

tions are also good choices. For patients' initial rehabilitation in the clinic, medications should be flexibly chosen according to the individual difference and susceptibility test results.

Disk tests can be read with all *Candida* species after the first 24 h of incubation: In vitro antifungal activity points with the disk test as a screening procedure. Our study indicated that both *C. albicans* isolates were susceptible to Amphotericin-B (20 µg). Nearly both *C. albicans* isolates show a different range of resistance (3-5mm) to fluconazole, followed by clotrimazole, Ketoconazole, Itraconazole (10 µg), and voriconazole as presented in Table 2. Among the antifungal discs, the lowest inhibition zone was recorded for fluconazole. Numerous studies have measured the incidence of clinical fluconazole resistance from 6 – 36%, 15%, and 5–10% (39). Our results are consistent with those reported Mohamadi *et al.* (2015), who recorded that the resistance to fluconazole, Itraconazole, ketoconazole, clotrimazole, voriconazole, posaconazole, Nystatin, and amphotericin B was 76%, 62%, 72%, 55%, 6%, 7%, 1%, and 0% (40).

The scientific community, like the practitioners of the food industry, has provoked the hunt for antimicrobial alternatives to fight the ongoing development of bacterial strains resistant to multiple antibiotics. Silver, often regarded as a broad-spectrum antimicrobial agent, may therefore be a suitable option, particularly in its nano-form (41). The various N.P.s were talented to constrain the bacterial progress at diverse concentrations. The MIC in both methods (micro-dilution and well diffusion methods) for Ag 90nm were 2500 µg/ml 13.5mm and 2500 µg/ml 12mm. It indicates that silver nanoparticles possess antibacterial action against *Salmonella typhimurium* as shown in Table 3. Kumar *et al* (2012) reported an excellent antimicrobial activity of silver nanoparticles (10–100) nm against five clinical pathogenic bacteria (*S. typhi*, *E. coli*, *Klebsiella pneumoniae*, *S. aureus*, and *Vibrio cholerae*) (42). Silver nanoparticles are well known for their antimicrobial activities against a wide range of pathogenic organisms (43).

Contrary, moderate antimicrobial action was observed in the *S. typhi* (44), which agrees with the results of the present research. On the other hand, AgNPs are an effective antibiotic against *S. epidermidis*, *S. aureus*, *E. coli*, and *S. typhi* (45). In contrast, Zarei *et al.* (2014) reported that Ag NPs displayed antimicrobial activity against a single strain of *S. Typhimurium* grown in tryptone soya broth at 35C, reporting a MIC of 3.12mg/mL and an MBC of 6.25mg/mL (46); the values of MIC and

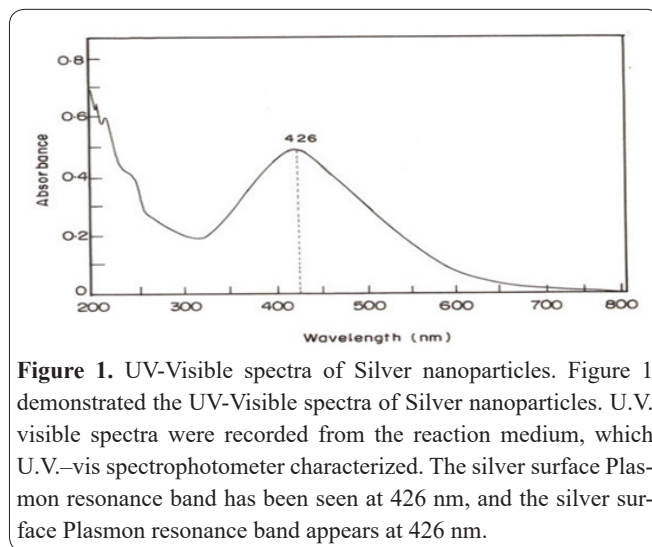


Figure 1. UV-Visible spectra of Silver nanoparticles. Figure 1 demonstrated the UV-Visible spectra of Silver nanoparticles. U.V. visible spectra were recorded from the reaction medium, which U.V.–vis spectrophotometer characterized. The silver surface Plasmon resonance band has been seen at 426 nm, and the silver surface Plasmon resonance band appears at 426 nm.

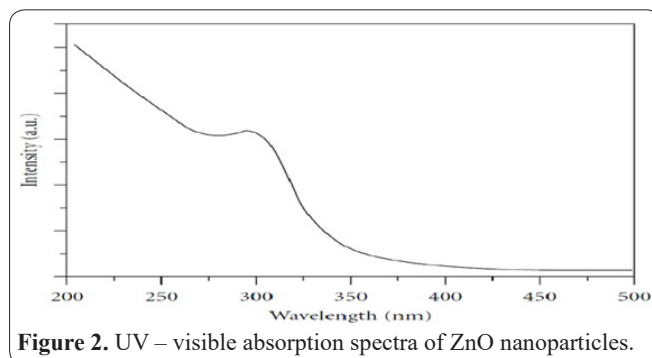


Figure 2. UV – visible absorption spectra of ZnO nanoparticles.

MBC are lower than those reported in the present study. This may, in part, be due to the lesser size of the Ag NPs used in their study (10 nm) compared to the average size in this study (20 nm) or differences in NP Dissolution behavior.

The silver nanoparticles showed a maximum absorption band at 430 nm, indicating that the nanoparticles were scattered in the aqueous solution, preventing the AgNPs from agglomeration in UV-Vis (Figure 1). UV-Vis profile of AgNPs exposed a peak at 400 nm, which matches the typical surface plasmon resonance of AgNPs. The ZnO nanoparticles' absorption band demonstrated a blue shift (from 275 nm to 350 nm) due to the quantum confinement of the excitons present in the sample. The quantum size effect of these nanoparticles is indicated by this optical phenomenon shown in Figure 2.

Figure 3 represents the FT-IR spectrum of TiO₂. Various characteristics peaks are shown. The absorption band range was 3454.51cm⁻¹, and it is related to

Table 3. Minimum Inhibition concentration (ug/ml) and Inhibition zone (mm) of antibacterial activity of Nanoparticle against *Salmonella* spp.

Nanoparticle	Bacteria Isolates			
	S1		S2	
	MIC (µg/ml)	Inhibition zone (mm)	MIC (µg/ml)	Inhibition zone (mm)
Ag-90nm	2500	13.5	2500	12
ZnO-20nm	1250	15.5	625	14
ZnO-50nm	2500	14	1250	15
TiO ₂ -10nm	5000	11	2500	13
TiO ₂ -50nm	5000	13	2500	15
Normal saline	0	0	0	0

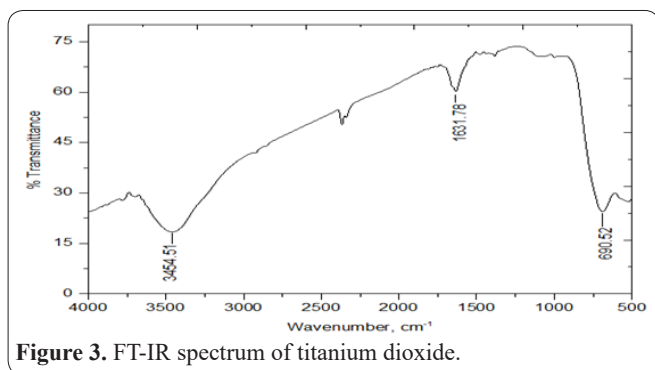


Figure 3. FT-IR spectrum of titanium dioxide.

stretching. 1631.78 cm^{-1} to bending O-H vibration, demonstrating the water as moisture. The intense characteristics peak of TiO_2 was seen at 690.52 cm^{-1} , and it is also assigned to the Ti-O stretching band (47).

Information of chemical bonding between Zn and O is shown in Fig.4. The spectrum shown in the figure demonstrated a broad peak around 457 cm^{-1} and shoulder around 545 cm^{-1} , corresponding ZnO nanoparticles—comparatively, and other ranges showed a smooth peak.

Figure 5 shows Fourier transform-infrared spectra of silver nanoparticles. FTIR spectral absorption peaks were at 773, 800, 813, 1040, 1288, 1530, and 3226/ cm in the region 500–4000/ cm (Figure 5). The biomolecules and their different functional groups have been seen through FTIR analysis.

Figure 6 well-defined the optical absorption spectra of TiO_2 nanoparticles. TiO_2 nanoparticles appear transparent in the visible region. A sharp absorbance peak around 2.93 eV has also been observed. The value $n=1/2$ does not appear to be meaningful for data of the band-gap energy, indicating that TiO_2 is a direct bandgap type semiconductor.

Antimicrobial activity of ZnO NPs has been shown on *Salmonella spp.* (48). The Zinc oxide 20 nm had the feature of its MIC average at (1250 $\mu\text{g}/\text{ml}$, 625 $\mu\text{g}/\text{ml}$) showed 15,5 and 14mm, respectively, in the micro-broth technique. The inhibition zones of ZnO 50 nm showed phenotypic inhibition zone at average 14mm,15 mm on agar plate, and MIC average about 2500,1250 $\mu\text{g}/\text{ml}$, respectively, as represented in Table 3. Lastly, the isolates presented sensitivity to ZnO (20-50) nm in MIC ranged (156.25-1250) $\mu\text{g}/\text{ml}$. The inhibition zone was (10-18) mm. The ZnO N.P.s (5 μg mLG1) gave a remarkable mean inhibition zone diameter (IZD) of 18 ± 1.02 , 16 ± 0.08 , 08 ± 0.82 , 20 ± 1.04 and 22 ± 1.08 mm for *P. aeruginosa*, *E. coli*, *S. enteritidis*, *K. pneumoniae*, and *P. mirabilis*, respectively (49).

Numerous mechanisms have been suggested to elucidate the antibacterial properties of ZnO nanoparticles. The formation of hydrogen peroxide from the surface of ZnO is considered an effective means of inhibiting bacterial development (50). The release of Zn^{2+} ions, which prefer to disrupt the cell membrane lipids and proteins, resulted in the leakage of intracellular contents and, eventually, cell death is another possible mechanism for ZnO antibacterial activity (51). Other researchers approve the important antibacterial activity of ZnO nanoparticles wherein the nanoparticles might entirely lyse *S. typhimurium* and *S. aureus*, causing food poisoning (52). In a study carried out by Duffy *et al.* (2018), the MIC was reported for the five *Salmonella*

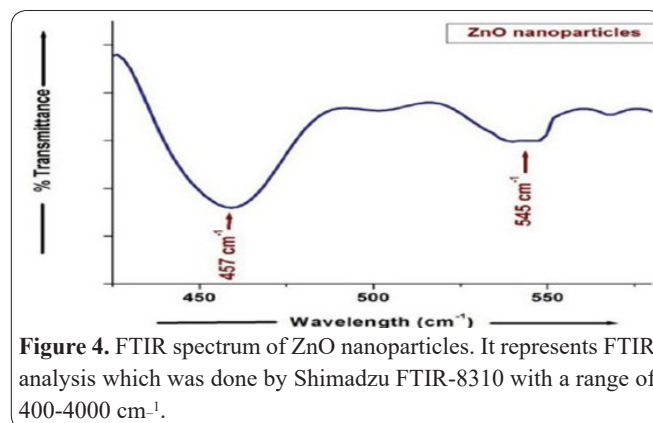


Figure 4. FTIR spectrum of ZnO nanoparticles. It represents FTIR analysis which was done by Shimadzu FTIR-8310 with a range of 400–4000 cm^{-1} .

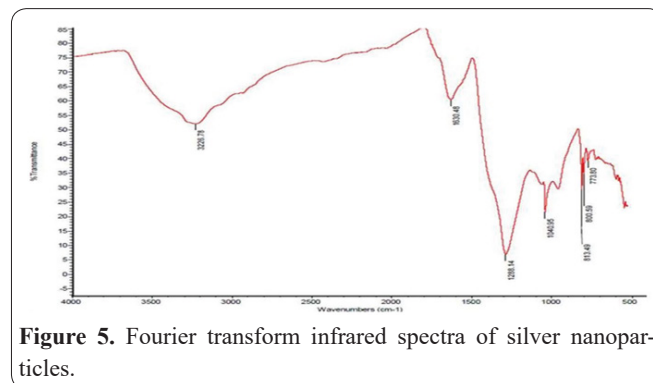


Figure 5. Fourier transform infrared spectra of silver nanoparticles.

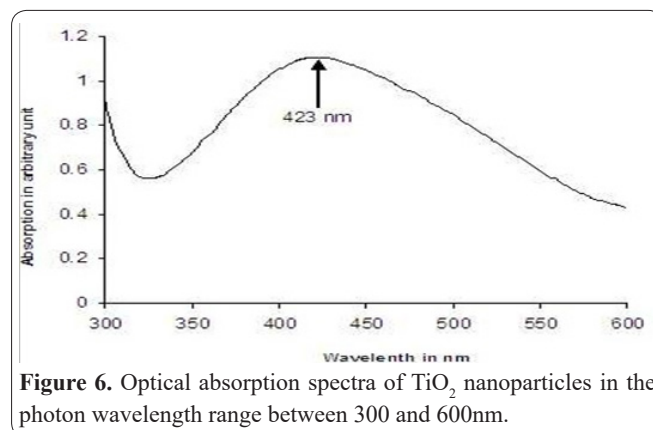


Figure 6. Optical absorption spectra of TiO_2 nanoparticles in the photon wavelength range between 300 and 600nm.

strains (312.5 $\mu\text{g}/\text{ml}$ 625 $\mu\text{g}/\text{ml}$), indicating lower effective treatment of *Salmonella* than our study (53). Tayel *et al.* (2011) used ZnO NPs of similar particle size (50 nm) to the current study, the nutrient broth was the incubation media used for the *S. Enteritidis*, and *S. Typhimurium* strains (54). However, their results were lower than that ours.

On the other hand, based on MIC, the antimicrobial effect of the TiO_2 nanoparticles, depending on the isolates' sensitivity to TiO_2 20 nm, was (1250–5000) $\mu\text{g}/\text{ml}$. The average inhibition zones were (11–14) mm, whereas the isolates presented average phenotypic inhibition zone (11–15) mm on an agar plate at an average MIC of about (1250–5000) $\mu\text{g}/\text{ml}$ for TiO_2 50 nm. Pan *et al.* (2010) describe some mechanisms of toxicity effects of NPs such as the TiO_2 (40–60) nm (8 and 80) ng/ml and ZnO (25–40) nm (8 and 80) ng/ml against bacteria which have weak mutagenic potential that induces frameshift mutation in *Salmonella typhimurium* (55).

TiO_2 nanoparticles are interesting subjects for microbial studies because of their specific characterization as size, shape, and structure of TiO_2 nanomaterials crystal, surface stability, and the transferences between different

phases of TiO₂ under stress and heat. TiO₂ Nano-materials were known as the glamour of recent medical research due to their microbicidal effect on other disease-causing organisms (56). The bactericidal effect of TiO₂ nanoparticles on bacteria is of extreme importance due to pathogenic bacteria's ability to enter an ecosystem's food chain (55,57). Mutagenicity evaluation of metal oxide nanoparticles by the bacterial reverse mutation assay.

If the concentration of TiO₂ increases, the inhibition zone also increased as per the measurements described by the inhibition zone. Nanomaterials are well known to show strong inhibiting effects against a wide range of bacterial strains. According to numerous studies, it is believed that the metal oxides convey the positive charge while the microorganisms have negative charges; this causes electromagnetic attraction between microorganisms and the metal oxides, which leads to oxidization and, finally, microorganisms' death (57).

The isolated *Brucella abortus* (B1 B2) showed sensitivity to NPs with the different MIC (5000 µg/ml) for Ag-90nm and inhibition zone of 12 mm. However, with a MIC of 2500(µg/ml), the inhibition zone was 13.5 mm. The ZnO-20nm MIC of 156.25(µg/ml) had an inhibition zone of 15.5 mm, and the MIC of 312.5(µg/ml) had an inhibition zone of 18 mm. Also, the ZnO-50nm MIC of 625(µg/ml) had an inhibition zone of 10 mm, and the MIC of 1250(µg/ml) had an inhibition zone of 11 mm. TiO₂-10nm with MIC of 5000(µg/ml) had an inhibition zone of 12 mm, and MIC of 2500(µg/ml) had an inhibition zone of 11 mm. Nevertheless, TiO₂-50nm with MIC of 2500(µg/ml) had an inhibition zone of 11 mm, and MIC of 2500(µg/ml) had an inhibition zone of 13 mm, as shown in Table 4.

Numerous studies demonstrated that AgNP activity is proportional to its size (57,58). It was found that AgNPs of smaller dimensions can penetrate bacteria (59). Our result revealed that silver nanoparticles have an instant antimicrobial impact on intramacrophage *B. abortus*. A study recorded that silver nanoparticles have an antimicrobial impact on intramacrophage *B. abortus* 544 (60). MBC, MIC, and experiments at two ppm and one ppm of silver nanoparticle concentrations have shown that silver nanoparticles have an antimicrobial effect against intramacrophage *B. abortus* 544 over 24 hours and have shown that silver nanoparticles have an antimicrobial effect against intramacrophage *B. abortus* 544 and may therefore be useful for brucellosis care.

In the current study, ZnO nanoparticles prevented the growth of bacterial isolates. The tested isolates are vulnerable to more than the MIC of ZnO nanoparticles than high resistance to multiple routine antibiotics classes. Jiang *et al.* (2008) described the antimicrobial action of ZnO nanoparticles against food-related bacteria (61). Various mechanisms have been described for the antimicrobial activity of ZnO nanoparticles. The hydrogen peroxide generation and Zn²⁺ ions release have the ability of cell membrane and intracellular contents damage. Also, by reducing the particle size of nanoparticles and increasing surface area, the antimicrobial properties of the ZnO will rise.

Haghi *et al.* (2012) has shown that 150 mg/ml of TiO₂ and 200 mg/ml of TiO₂ have the best effect on this study's seven bacterial isolates, while 50 mg/ml of TiO₂ and 100 mg/ml of TiO₂ have a little antibacterial effect on half of them (62).

TiO₂ nanoparticles with 1-100nm diameter are interesting to investigators because of specific properties such as size, shape, and structure of TiO₂ nanomaterials crystal, surface stability, and the transferences between different phases TiO₂ under stress and heat. TiO₂ Nano-materials were known as recent medical research glamour due to their microbicidal effect on other disease-causing organisms (56). The bactericidal effect of TiO₂ nanoparticles on bacteria is of great importance due to pathogenic bacteria's ability to enter an ecosystem's food chain (57). The minimum inhibition concentration (ug/ml) and inhibition zone (mm) of antibacterial activity of nanoparticles against *Brucella* spp have been shown in (Table 4). In the expansion of novel nanodevices which can be used in many physical, biological, biomedical, and pharmaceutical applications nanosized inorganic

Table 4. Minimum inhibition concentration (ug/ml) and inhibition zone (mm) of antibacterial activity of nanoparticles against *Brucella* spp.

Nanoparticle	Bacteria Isolates			
	B1		B2	
	MIC (µg/ml)	Inhibition zone (mm)	MIC (µg/ml)	Inhibition zone (mm)
Ag-90nm	5000	12	2500	13.5
ZnO-20nm	156.25	15.5	312.5	18
ZnO-50nm	625	10	1250	11
TiO ₂ -10nm	5000	12	2500	11
TiO ₂ -50nm	2500	11	2500	13
Normal saline	0	0	0	0

Table 5. Minimum Inhibition concentration (µg/ml) and Inhibition zone (mm) of antibacterial activity of Nanoparticle against *Candida albicans*.

Nanoparticle	Bacteria Isolates			
	C1		C2	
	MIC (µg/ml)	Inhibition zone (mm)	MIC (µg/ml)	Inhibition zone (mm)
Ag-90nm	1250	12	2500	12
ZnO-20nm	625	15.5	312.5	14
ZnO-50nm	1250	14	625	18
TiO ₂ -10nm	2500	13	5000	14
TiO ₂ -50nm	1250	13	2500	12
Normal saline	0	0	0	0

particles are recognized as a progressively important material (63). The MIC and MFC values varied between 2500 µg/ml and 625 µg g/mL and showed inhibition zone ranged 11-15,5 mm respectively as in Table 5.

This research investigated the antifungal activity of nano-Ag against *C. albicans*. Antifungal activity of Nano-Ag towards fungal strains compared to amphotericin B's antifungal activity in the zone inhibition values is also tested. Kim *et al.* (2009) reported that nano-Ag has remarkable antifungal potency in treating fungal infectious diseases (64). Herrera *et al.* (2001) represent nano-Ag as a proper antimicrobial agent, mainly because it is highly toxic to most microorganisms (65). Endo *et al.* (1997) have reported that the inhibition of bud growth relates to membrane damage (66). This report suggests that probably due to membrane integrity destruction, nano-Ag could inhibit the normal budding process.

the results obtained in this study demonstrate the importance of the N.P.s size, as the lowest nanoparticles bring the highest inhibition (67). Lara *et al.* (2015) presented that biofilm uncovered to AgNPs shows a few *Candida albicans* filamentous formations (68).

There is incidental evidence that these particles have good antimicrobial activity (69). The AgNPs have shown multiple antimicrobial activities against a wide array of microorganisms, possibly because of multiple mechanisms involved in its antimicrobial action, including activity against drug-resistant bacteria, fungi, and viruses (70). Since significant differences in terms of sufficient size and concentration, the action was observed for the three investigated pathogens. This may be attributed to many features strictly related to each strain's genetic features, including the presence of specific genetic determinants of resistance (71).

Fayaz *et al.* (2012) showed that the AgNPs-coated condom has antiviral, antibacterial, and anti-fungi (against *Candida* spp.) properties (72). This suggests that AgNPs can treat all multi-drug resistant pathogens of diverse types from all clinical sources.

According to the findings, the AgNPs solution has fungistatic and fungicidal effects against the microorganism tested. It also suggests that it can be suitable to develop new antimicrobial agents with multiple biomedical field applications. The inhibition zone formed around *C. Albicans* was slightly further than that of the other two organisms when AgNps was used alone.

The fungicidal effects of ZnO-NP treatments, such as ZnO nanocomposites and ZnO, have recently been established (28). ZnO-NP has also been reported to exhibit inhibitory effects on bacterial biofilm formation and candidal biofilm formation (73). Consequently, evaluated the antimicrobial effects of ZnO on *C. albicans*) MICs of ZnO (5-50) µg/mL against isolates were also done by but less than our results (74).

Our results are in discrepancy with those reported by Daou *et al.* (2017), who demonstrated that TiO₂-ZnO allowed complete eradication of *C. albicans* with very low MIC (75). On the other hand, the study found that the least inhibition zone of *C. albicans* was 8 mm in concentration 0.01 mg/ml of ZnO by Suha *et al.* (2015) in contrast to the results of Yousef *et al.* (2012) who showed that the best inhibition zone of *C. albicans* was 18 mm in concentration 10 µg/ml which is equal to 0.01 mg/ml the least concentration (76,77). Several studies

have described the germicidal mechanisms of TiO₂ nanoparticles involving the release of positively charged ions to reaction medium linked to (negative charges) thiol group (-S.H.) of the proteins on the cytoplasmic membrane (78). This response led to the imprisonment of the cell wall and augmented permeability. It deforms cellular components such as DNA, ribosomes, cellular enzymes, and microbial cell (79). So far, many studies have been conducted on the role of nanoparticles in the biological field (80-88). In this regard, it is best to study the relationship between the use of nanoparticles and some abnormalities and complications, such as genetic polymorphisms (89), mitochondrial diseases (90), sexual disorders (91) and overall human health (92) Impact.

Acknowledgments

None

Interest conflict

The authors declare no conflict of interest.

References

1. Vert M, Doi Y, Hellwich KH, Hess M, Hodge P, Kubisa P, et al. Terminology for biorelated polymers and applications (IUPAC recommendations 2012). *Pure Appl Chem* 2012;84:377–410.
2. Gold K, Slay B, Knackstedt M, Gaharwar AK. Antimicrobial Activity of Metal and Metal-Oxide Based Nanoparticles. *Adv Ther* 2018;1:1700033.
3. Kadiyala U, Kotov NA, VanEpps JS. Antibacterial Metal Oxide Nanoparticles: Challenges in Interpreting the Literature. *Curr Pharm Des* 2018;24:896–903.
4. Organization WH. Foodborne diseases, emerging. Fact sheet no. 124 2002.
5. Threlfall EJ, Ward LR, Skinner JA, Rowe B. Increase in multiple antibiotic resistance in nontyphoidal salmonellas from humans in england and wales: A comparison of data for 1994 and 1996. *Microb Drug Resist* 1997;3:263–6.
6. Cruchaga S, Echeita A, Aladueña A, García-Peña J, Frias N, Usera MA. Antimicrobial resistance in salmonellae from humans, food and animals in Spain in 1998. *J Antimicrob Chemother* 2001;47:315–21.
7. Helms M, Vastrup P, Gerner-Smidt P, Mølbak K. Excess mortality associated with antimicrobial drug-resistant *Salmonella typhimurium*. *Emerg Infect Dis* 2002;8:490–5.
8. Ryan CA, Nickels MK, Hargrett Bean NT, Potter ME, Endo T, Mayer L, et al. Massive Outbreak of Antimicrobial-Resistant Salmonellosis Traced to Pasteurized Milk. *JAMA J Am Med Assoc* 1987;258:3269–74.
9. Van Bambeke F, Barcia-Macay M, Lemaire S, Tulkens PM. Cellular pharmacodynamics and pharmacokinetics of antibiotics: Current views and perspectives. *Curr Opin Drug Discov Dev* 2006;9:218–30.
10. Pappas G, Solera J, Akritidis N, Tsianos E. New approaches to the antibiotic treatment of brucellosis. *Int J Antimicrob Agents* 2005;26:101–5.
11. McManus BA, Coleman DC. Molecular epidemiology, phylogeny and evolution of *Candida albicans*. *Infect Genet Evol* 2014;21:166–78.
12. Javad G, Taheri Sarvtin M, Hedayati MT, Hajheydari Z, Yazdani J, Shokohi T. Evaluation of candida colonization and specific humoral responses against candida albicans in patients with atopic dermatitis. *Biomed Res Int* 2015;2015:e555–60.

13. Çetin BŞ. European guideline for the management of scabies. *Cocuk Enfeksiyon Derg* 2017;11:107–9.
14. Hoshi N, Mori H, Taguchi H, Taniguchi M, Aoki H, Sawada T, et al. Management of oral candidiasis in denture wearers. *J Prosthodont Res* 2011;55:48–52.
15. Weissig V, Pettinger TK, Murdock N. Nanopharmaceuticals (part 1): products on the market. *Int J Nanomedicine* 2014;9:4357.
16. Oves M, Aslam M, Rauf MA, Qayyum S, Qari HA, Khan MS, et al. Antimicrobial and anticancer activities of silver nanoparticles synthesized from the root hair extract of *Phoenix dactylifera*. *Mater Sci Eng C* 2018;89:429–43.
17. Sirelkhatim A, Mahmud S, Seeni A, Kaus NHM, Ann LC, Bakhori SKM, et al. Review on zinc oxide nanoparticles: Antibacterial activity and toxicity mechanism. *Nano-Micro Lett* 2015;7:219–42.
18. Rappaport F, Konforti N, Navon B. A new enrichment medium for certain salmonellae. *J Clin Pathol* 1956;9:261.
19. Ligozzi M, Bernini C, Bonora MG, De Fatima M, Zuliani J, Fontana R. Evaluation of the VITEK 2 system for identification and antimicrobial susceptibility testing of medically relevant gram-positive cocci. *J Clin Microbiol* 2002;40:1681–6.
20. MacFaddin JF. *Biochemical tests for identification of medical bacteria* 2000.
21. Roberts GD, Wang HS, Hollick GE. Evaluation of the API 20 C microtube system for the identification of clinically important yeasts. *J Clin Microbiol* 1976;3:302–5.
22. Liu Z guo, Di D dong, Wang M, Liu R hong, Zhao H yan, Piao D ri, et al. In vitro antimicrobial susceptibility testing of human *Brucella melitensis* isolates from Ulanqab of Inner Mongolia, China. *BMC Infect Dis* 2018;18:1–6.
23. Wikler M, Cockerill F, Craig W, Dudley M, Eliopoulos G, Hecht D. Performance Standards for Antimicrobial Susceptibility Testing; Seventeenth Informational Supplement. *Clin Lab Standars Inst - NCCLS* 2007;27:1–182.
24. Ansari MA, Khan HM, Khan AA, Sultan A, Azam A. Synthesis and characterization of the antibacterial potential of ZnO nanoparticles against extended-spectrum β -lactamases-producing *Escherichia coli* and *Klebsiella pneumoniae* isolated from a tertiary care hospital of North India. *Appl Microbiol Biotechnol* 2012;94:467–77.
25. Gardea-Torresdey JL, Gomez E, Peralta-Videa JR, Parsons JG, Troiani H, Jose-Yacamán M. Alfalfa sprouts: A natural source for the synthesis of silver nanoparticles. *Langmuir* 2003;19:1357–61.
26. Sadiq IM, Chowdhury B, Chandrasekaran N, Mukherjee A. Antimicrobial sensitivity of *Escherichia coli* to alumina nanoparticles. *Nanomedicine Nanotechnology, Biol Med* 2009;5:282–6.
27. Saginur R, St. Denis M, Ferris W, Aaron SD, Chan F, Lee C, et al. Multiple combination bactericidal testing of staphylococcal biofilms from implant-associated infections. *Antimicrob Agents Chemother* 2006;50:55–61.
28. Wagay S, Dwivedi S, Sharma M, Tripathi J, Ahmad M. Antimicrobial activity of *Catharanthus roseus*. *Chem Mater Res* 2013;3:61–4.
29. Fakhra S, Shilpa S. Synthesis of silver nanoparticles using *Cos-tusspeciosus* and study of its anti-microbial properties against urinary tract pathogens. *Int J Curr Microbiol Appl Sci* 2014;3:248–52.
30. Arora DS, Kaur GJ. Antibacterial activity of some Indian medicinal plants. *J Nat Med* 2007;61:313–7.
31. Panhotra BR, Saxena AK, Al-Arabi Al-Ghamdi AM. Emerging nalidixic acid and ciprofloxacin resistance in non-typhoidal *Salmonella* isolated from patients having acute diarrhoeal disease. *Ann Saudi Med* 2004;24:332–6.
32. &NA; a Nosocomial Outbreak of Fluoroquinolone-Resistant *Salmonella* Infection. *Infect Dis Clin Pract* 2001;10:293–4.
33. Nakaya H, Yasuhara A, Yoshimura K, Oshihoi Y, Izumiya H, Watanabe H. Life-threatening infantile diarrhea from fluoroquinolone-resistant *Salmonella enterica* Typhimurium with mutations in both *gyrA* and *parC*. *Emerg Infect Dis* 2003;9:255–7.
34. Cooke RPD, Perrett L. Antimicrobial susceptibility data for *Brucella melitensis* isolates cultured from UK patients. *J Infect* 2014;68:401.
35. Gattringer KB, Suchomel M, Eder M, Lassnigg AM, Graninger W, Presterl E. Time-dependent effects of rifampicin on staphylococcal biofilms. *Int J Artif Organs* 2010;33:621–6.
36. Sandalakis V, Psaroulaki A, De Bock PJ, Christidou A, Gevaert K, Tsiotis G, et al. Investigation of rifampicin resistance mechanisms in *Brucella abortus* using MS-driven comparative proteomics. *J Proteome Res* 2012;11:2374–85.
37. Eumkeb G, Sakdarat S, Siriwong S. Reversing β -lactam antibiotic resistance of *Staphylococcus aureus* with galangin from *Alpinia officinarum* Hance and synergism with ceftazidime. *Phytomedicine* 2010;18:40–5.
38. Skalsky K, Yahav D, Bishara J, Pitlik S, Leibovici L, Paul M. Treatment of human brucellosis: Systematic review and meta-analysis of randomised controlled trials. *Bmj* 2008;336:701–4.
39. Enwuru CA, Ogunledun A, Idika N, Enwuru N V, Ogbonna E, Aniedobe M, et al. Fluconazole resistant opportunistic oro-pharyngeal candida and non-candida yeast-like isolates from HIV infected patients attending ARV clinics in Lagos, Nigeria. *Afr Health Sci* 2008;8:142–8.
40. Mohamadi J, Havasian MR, et al. Antifungal drug resistance pattern of *Candida* spp isolated from vaginitis in Ilam-Iran during 2013-2014. *Bioinformatics* 2015;11:203–6.
41. Kalishwaralal K, BarathManiKanth S, Pandian SRK, Deepak V, Gurunathan S. Silver nanoparticles impede the biofilm formation by *Pseudomonas aeruginosa* and *Staphylococcus epidermidis*. *Colloids Surfaces B Biointerfaces* 2010;79:340–4.
42. Kumar P, Selvi Senthamil S, Prabha Lakshmi A, Selvaraj M, Rani Macklin L, Suganthi P, et al. Antibacterial activity and in-vitro cytotoxicity assay against brine shrimp using silver nanoparticles synthesized from *Sargassum ilicifolium*. *Dig J Nanomater Biostructures* 2012;7:1447–55.
43. Shrivastava S, Bera T, Roy A, Singh G, Ramachandrarao P, Dash D. Characterization of enhanced antibacterial effects of novel silver nanoparticles. *Nanotechnology* 2007;18:225103.
44. Nanda A, Saravanan M. Biosynthesis of silver nanoparticles from *Staphylococcus aureus* and its antimicrobial activity against MRSA and MRSE. *Nanomedicine Nanotechnology, Biol Med* 2009;5:452–6.
45. Jain J, Arora S, Rajwade JM, Omray P, Khandelwal S, Paknikar KM. Silver nanoparticles in therapeutics: Development of an antimicrobial gel formulation for topical use. *Mol Pharm* 2009;6:1388–401.
46. Zarei M, Jamnejad A, Khajehali E. Antibacterial effect of silver nanoparticles against four foodborne pathogens. *Jundishapur J Microbiol* 2014;7.
47. Ba-Abbad MM, Kadhum AAH, Mohamad AB, Takriff MS, Sopian K. Synthesis and catalytic activity of TiO₂ nanoparticles for photochemical oxidation of concentrated chlorophenols under direct solar radiation. *Int J Electrochem Sci* 2012;7:4871–88.
48. Soren S, Kumar S, Mishra S, Jena PK, Verma SK, Parhi P. Evaluation of antibacterial and antioxidant potential of the zinc oxide nanoparticles synthesized by aqueous and polyol method. *Microb Pathog* 2018;119:145–51.
49. Maduabuchi EK, Siwe-Nound X. Green Synthesis of Zinc Oxide Nanoparticles and Their Antibiotic-potential Activities of Mucin Against Pathogenic Bacteria. *Res J Nanosci Nanotechnol* 2019;10:9–14.
50. Liu Y, He L, Mustapha A, Li H, Hu ZQ, Lin M. Antibacte-

- rial activities of zinc oxide nanoparticles against *Escherichia coli* O157:H7. *J Appl Microbiol* 2009;107:1193–201.
51. Jin T, Sun D, Su JY, Zhang H, Sue HJ. Antimicrobial efficacy of zinc oxide quantum dots against *Listeria monocytogenes*, *Salmonella* Enteritidis, and *Escherichia coli* O157:H7. *J Food Sci* 2009;74:M46–52.
 52. Nazoori ES, Kariminik A. In vitro evaluation of antibacterial properties of zinc oxide nanoparticles on pathogenic prokaryotes. *J Appl Biotechnol Reports* 2018;5:162–5.
 53. Duffy LL, Osmond-McLeod MJ, Judy J, King T. Investigation into the antibacterial activity of silver, zinc oxide and copper oxide nanoparticles against poultry-relevant isolates of *Salmonella* and *Campylobacter*. *Food Control* 2018;92:293–300.
 54. Tayel AA, El-Tras WF, Moussa S, El-Baz AF, Mahrous H, Salem MF, et al. Antibacterial action of zinc oxide nanoparticles against foodborne pathogens. *J Food Saf* 2011;31:211–8.
 55. Pan X, Redding JE, Wiley PA, Wen L, McConnell JS, Zhang B. Mutagenicity evaluation of metal oxide nanoparticles by the bacterial reverse mutation assay. *Chemosphere* 2010;79:113–6.
 56. Zallen R, Moret MP. The optical absorption edge of brookite TiO₂. *Solid State Commun* 2006;137:154–7.
 57. Zhang H, Chen G. potent antibacterial activities of Ag/TiO₂ nanocomposite powders synthesized by a one-pot sol-gel method. *Environ Sci Technol* 2009;43:2905–10.
 58. Tamayo LA, Zapata PA, Vejar ND, Azócar MI, Gulppi MA, Zhou X, et al. Release of silver and copper nanoparticles from polyethylene nanocomposites and their penetration into *Listeria monocytogenes*. *Mater Sci Eng C* 2014;40:24–31.
 59. Wu D, Fan W, Kishen A, Gutmann JL, Fan B. Evaluation of the antibacterial efficacy of silver nanoparticles against *Enterococcus faecalis* biofilm. *J Endod* 2014;40:285–90.
 60. Alizadeh H, Salouti M, Shapouri R. Bactericidal effect of silver nanoparticles on intramacrophage *Brucella abortus* 544. *Jundishapur J Microbiol* 2014;7.
 61. Jiang W, Mashayekhi H, Xing B. Bacterial toxicity comparison between nano- and micro-scaled oxide particles. *Environ Pollut* 2009;157:1619–25.
 62. Haghi M, Hekmatfashar M, Janipour MB, Gholizadeh SS, Faraz MK, Sayyadifar F, et al. Antibacterial effect of TiO₂ nanoparticles on pathogenic strain of *E. coli*. *Int J Adv Biotechnol Res* 2012;3:621–4.
 63. Chan WCW, Maxwell DJ, Gao X, Bailey RE, Han M, Nie S. Luminescent quantum dots for multiplexed biological detection and imaging. *Curr Opin Biotechnol* 2002;13:40–6.
 64. Kim KJ, Sung WS, Suh BK, Moon SK, Choi JS, Kim JG, et al. Antifungal activity and mode of action of silver nano-particles on *Candida albicans*. *BioMetals* 2009;22:235–42.
 65. Herrera Costa F, Narana Ribeiro El Achkar V, Costa V, Paladini I, Kowalski LP, Rodarte Carvalho Y, et al. Different Expression of Aldehyde Dehydrogenases 1A1 and 2 in Oral Leukoplakia With Epithelial Dysplasia and in Oral Squamous Cell Carcinoma. *Appl Immunohistochem Mol Morphol* 2019;27:537–42.
 66. Endo M, Takesako K, Kato I, Yamaguchi H. Fungicidal action of aureobasidin A, a cyclic depsipeptide antifungal antibiotic, against *Saccharomyces cerevisiae*. *Antimicrob Agents Chemother* 1997;41:672–6.
 67. Kumar S, Bhattacharya W, Singh M, Halder D, Mitra A. Plant latex capped colloidal silver nanoparticles: A potent anti-biofilm and fungicidal formulation. *J Mol Liq* 2017;230:705–13.
 68. Lara HH, Romero-Urbina DG, Pierce C, Lopez-Ribot JL, Arellano-Jiménez MJ, Jose-Yacamán M. Effect of silver nanoparticles on *Candida albicans* biofilms: An ultrastructural study. *J Nanobiotechnology* 2015;13:1–12.
 69. Kim JS, Kuk E, Yu KN, Kim JH, Park SJ, Lee HJ, et al. Antimicrobial effects of silver nanoparticles. *Nanomedicine Nanotechnology, Biol Med* 2007;3:95–101.
 70. Sondi I, Salopek-Sondi B. Silver nanoparticles as antimicrobial agent: A case study on *E. coli* as a model for Gram-negative bacteria. *J Colloid Interface Sci* 2004;275:177–82.
 71. Lara HH, Ayala-Núñez N V., del Turrent LCI, Padilla CR. Bactericidal effect of silver nanoparticles against multidrug-resistant bacteria. *World J Microbiol Biotechnol* 2010;26:615–21.
 72. Mohammed Fayaz A, Ao Z, Girilal M, Chen L, Xiao X, Kalai-chelvan PT, et al. Inactivation of microbial infectiousness by silver nanoparticles-coated condom: A new approach to inhibit HIV- and HSV-transmitted infection. *Int J Nanomedicine* 2012;7:5007–18.
 73. Vahedi M, Hosseini-Jazani N, Yousefi S, Ghahremani M. Evaluation of anti-bacterial effects of nickel nanoparticles on biofilm production by *Staphylococcus epidermidis*. *Iran J Microbiol* 2017;9:160–8.
 74. Monteiro DR, Silva S, Negri M, Gorup LF, de Camargo ER, Oliveira R, et al. Silver colloidal nanoparticles: Effect on matrix composition and structure of *Candida albicans* and *Candida glabrata* biofilms. *J Appl Microbiol* 2013;114:1175–83.
 75. Daou I, Zegaoui O, Moukrad N, Filali FR. Antimicrobial activity of ZnO-TiO₂ nanomaterials synthesized from three different precursors of ZnO: influence of ZnO/TiO₂ weight ratio. *Water Sci Technol* 2018;77:1238–49.
 76. M. Yousef J, N. Danial E. In *Vitro* Antibacterial Activity and Minimum Inhibitory Concentration of Zinc Oxide and Nano-particle Zinc oxide Against Pathogenic Strains. *Int J Heal Sci* 2012;2:38–42.
 77. Abd Suha T, Ali AF. Effect of zinc oxide nanoparticles on *Candida albicans* of human saliva (in vitro study). *Eur J Med* 2015:235–43.
 78. Jayaseelan C, Rahuman AA, Roopan SM, Kirthi AV, Venkatesan J, Kim SK, et al. Biological approach to synthesize TiO₂ nanoparticles using *Aeromonas hydrophila* and its antibacterial activity. *Spectrochim Acta - Part A Mol Biomol Spectrosc* 2013;107:82–9.
 79. Koseki H, Shirai K, Tsurumoto T, Asahara T, Baba K, Taoda H, et al. Bactericidal performance of photocatalytic titanium dioxide particle mixture under ultraviolet and fluorescent light: An in vitro study. *Surf Interface Anal* 2009;41:771–4.
 80. Khaledian S, Noroozi-Aghideh A, Kahrizi D, Moradi S, Abdoli M, Ghasemalian AH, Heidari MF. Rapid detection of diazinon as an organophosphorus poison in real samples using fluorescence carbon dots. *Inorg Chem Commun* 2021;130:108676.
 81. Darvishi E, Kahrizi D, Arkan E. Comparison of different properties of zinc oxide nanoparticles synthesized by the green (using *Juglans regia* L. leaf extract) and chemical methods. *J Mol Liq* 2019 Jul 15;286:110831.
 82. Khaledian S, Kahrizi D, Balaky ST, Arkan E, Abdoli M, Martinez F. Electrospun nanofiber patch based on gum tragacanth/polyvinyl alcohol/molybdenum disulfide composite for tetracycline delivery and their inhibitory effect on Gram+ and Gram–bacteria. *J Mol Liq* 2021;334:115989.
 83. Khaledian S, Kahrizi D, Moradi S, Martinez F. An experimental and computational study to evaluation of chitosan/gum tragacanth coated-natural lipid-based nanocarriers for sunitinib delivery. *J Mol Liq* 2021;334:116075.
 84. Rahimi T, Kahrizi D, Feyzi M, Ahmadvandi HR, Mostafaei M. Catalytic performance of MgO/Fe₂O₃-SiO₂ core-shell magnetic nanocatalyst for biodiesel production of *Camelina sativa* seed oil: Optimization by RSM-CCD method. *Ind Crops Prod* 2021;159:113065.
 85. Olfati A, Kahrizi D, Balaky ST, Sharifi R, Tahir MB, Darvishi E. Green synthesis of nanoparticles using *Calendula officinalis* extract from silver sulfate and their antibacterial effects on *Pectobacterium caratovorum*. *Inorg Chem Commun* 2021;125:108439.
 86. Moradi S, Khaledian S, Abdoli M, Shahlaei M, Kahrizi D. Nano-biosensors in cellular and molecular biology. *Cell Mol Biol*

2018;64(5):85-90.

87. Darvishi E, Kahrizi D, Arkan E, Hosseinabadi S, Nematpour N. Preparation of bio-nano bandage from quince seed mucilage/ZnO nanoparticles and its application for the treatment of burn. *J Mol Liq*. 2021;339:116598.

88. Mirmoeini T, Pishkar L, Kahrizi D, Barzin G, Karimi N. Phytotoxicity of green synthesized silver nanoparticles on *Camelina sativa* L. *Physiology and Molecular Biology of Plants*. 2021;27(2):417-27.

89. Ercisli M., Lechun, G, Azeez S, Hamasalih R, Song S, Aziziaran Z. Relevance of genetic polymorphisms of the human cytochrome P450 3A4 in rivaroxaban-treated patients. *Cell Mol Biomed Rep* 2021; 1(1): 33-41.

90. Aziziaran, Z., Bilal, I., Zhong, Y., Mahmood, A., Roshandel, M. Protective effects of curcumin against naproxen-induced mitochondrial dysfunction in rat kidney tissue. *Cell Mol Biomed Rep* 2021; 1(1): 23-32.

91. Kazemi E, Zargooshi J, Kaboudi M, Heidari P, Kahrizi D, Mahaki B, Mohammadian Y, Khazaei H, Ahmed K. A genome-wide association study to identify candidate genes for erectile dysfunction. *Brief Bioinforma* 2021;22(4):bbaa338. <https://doi.org/10.1093/bib/bbaa338>

92. Mojadadi A, Au A, Salah W, Witting P, Ahmad G. Role for selenium in metabolic homeostasis and human reproduction. *Nutrients* 2021;13(9):3256.